Inorg. Chem. **2004**, *43*, 2736–2744

Synthesis, Structures, and Magnetic Properties of Novel Mononuclear, Tetranuclear, and 1D Chain Mn^{III} Complexes Involving Three Related Asymmetrical Trianionic Ligands

Jean-Pierre Costes,* Françoise Dahan, Bruno Donnadieu, Maria-Jesus Rodriguez Douton,† Maria-Isabel Fernandez Garcia,† Azzedine Bousseksou, and Jean-Pierre Tuchagues

Laboratoire de Chimie de Coordination du CNRS, UPR 8241, liée par conventions à l'Université Paul Sabatier et à l'Institut National Polytechnique de Toulouse, 205 route de Narbonne, 31077 Toulouse Cedex, France

Received July 25, 2003

The manganese(III) complexes studied in this report derive from asymmetrical trianionic ligands abbreviated H_3L^i (i = 4–6). These ligands are obtained through reaction of salicylaldehyde with "half-units", the latter resulting from monocondensation of different diamines with phenylsalicylate,. Upon deprotonation, L^i (i = 4–6) possess an inner N_2O_2 coordination site with one amido, one imine, and two phenoxo functions, and an outer amido oxygen donor. The trianionic character of such ligands yields original neutral complexes with the L/Mn stoichiometry. The crystal and molecular structures of three complexes have been determined at 190 K (**1**) or 180 K (**2** and **3**). Complex **1** crystallizes in the triclinic space group $P\bar{1}$ (No. 2): a = 7.8582(14) Å, b = 10.9225(16) Å, c = 12.4882(18) Å, α = 67.231(14)°, β = 72.134(14)°, γ = 82.589(13)°, V = 940.6(3) Å^3, Z = 2. Complex **2** crystallizes in the orthorhombic space group *Pbcn* (No. 60): a = 23.8283(15) Å, b = 11.1605(7) Å, c = 26.152(2) Å, V = 6954.8(8) Å^3, Z = 8, while complex **3** crystallizes in the monoclinic space group $P2_1/c$ (No. 14) with a = 11.7443(14) Å, b = 7.5996(10) Å, c = 18.029(2) Å, β = 100.604(10)°, V = 1581.6(3) Å^3, Z = 4. Owing to hydrogen bonds and π–π stackings, the mononuclear neutral molecules of **1** are arranged in a 2D network while complexes **2** and **3** are tetranuclear and polymeric (1D chain) species, respectively, owing to the bridging ability of the oxygen atom of the amido function. The experimental magnetic susceptibilities of complexes **2** and **3** indicate the occurrence of similarly weak Mn^{III}–Mn^{III} antiferromagnetic interactions (J = –1.1 cm^{-1}). Single ion zero-field splitting of manganese(III) must be taken into account for satisfactorily fitting the data by exact calculation of the energy levels associated to the spin Hamiltonian through diagonalization of the full matrix for axial symmetry in **2** (J = – 1.1 cm^{-1}, D_1 = 2.2 cm^{-1}, D_2 = –2.8 cm^{-1}), D_1 and D_2 being associated to the six- and five-coordinate Mn ions, respectively. A weaker antiferromagnetic interaction (J = – 0.2 cm^{-1}) operates through π–π stacking in complex **1**. Complex **3** is a weak ferromagnet (ordering temperature ~7 K) as a result of the spin canting originating from the crystal packing.

Introduction

An investigation area of increasing importance in contemporary chemistry concerns functional materials made up from discrete molecules. Functionality depends on the electronic structure of the constituent molecules. In this regard, complexes of 3d transition metal ions provide a large variety of unusual electronic structures.[1] Dinuclear and polynuclear alkoxo-, phenoxo-, carboxylato-, and oxo-bridged manganese complexes are of current interest from a variety of viewpoints, including molecular magnetic materials and bioinorganic chemistry. In the former area, it has been shown that some of these polynuclear species possess large total spin values (S_T) in their ground state. Large S_T values provide the possibility of obtaining new manganese-based single-molecule magnets (SMMs).[2] In the area of bioinorganic chemistry, dinuclear and tetranuclear species may be used as synthetic models of the active site of various non-heme manganese proteins and enzymes such as catalases,[3]

* To whom correspondence should be addressed. E-mail: costes@lcc-toulouse.fr. Fax: 33 (0)5 61 55 30 03.

† Present address: Dpto de Quimica Inorganica, Universidad de Santiago de Compostela, Santiago de Compostela, E15782 Spain.

10.1021/ic0348796 CCC: $27.50
Published on Web 03/17/2004

liver arginase,[4] manganese ribonucleotide reductase (RNR),[5] thiosulfate oxidizing enzyme,[6] and the oxygen evolving complex (OEC) of photosystem 2.[7]

Important to the future of the above areas is the development of synthetic procedures that may yield new ligands from which polynuclear manganese species with original structure and properties may be obtained. Up to now, neutral manganese complexes have essentially been obtained by association of symmetrical neutral or mono- or dianionic ligands (the later two being most often Schiff bases) with halide, pseudohalide, carboxylato, hydroxo, and oxo anions in the metal coordination sphere.[8] This observation prompted us to extend the synthesis, through stepwise processes, of ligands including an inner asymmetrical trianionic tetradentate N_2O_2 coordination site with one amide, one imine, and two phenol functions, and an outer amido oxygen donor atom.

In this contribution, we describe the synthesis and full characterization of three such asymmetrical trianionic ligands, L^4H_3, L^5H_3, and L^6H_3, and the preparation, molecular structure, and magnetic properties of the complexes obtained by aerobic reaction of these ligands with manganese, $[L^6Mn(CH_3OH)_2]$, **1**, $[L^5{}_4Mn_4(H_2O)_2](CH_3OH)_2$, **2**, and $[L^4Mn(CH_3OH)]_n$, **3**.

Experimental Section

Materials. Phenyl salicylate, 1,2-diamino-2-methylpropane, 1,2-diaminopropane, 1,2-diaminoethane, salicylaldehyde, and $Mn(OAc)_2{\cdot}4H_2O$ (Aldrich) were used as purchased. High-grade solvents (propane-2-ol, dichloromethane, diethyl ether, acetone, ethanol, and methanol) were used for the syntheses of ligands and complexes.

Ligands. The method used to synthesize the half-unit trifunctional ligands L^iH_2 ($i = 1-3$) was adapted from the process described earlier.[9]

L^1H_2. A mixture of phenyl salicylate (2.14 g, 1×10^{-2} mol) and 1,2-diamino-2-methylpropane (0.88 g, 1×10^{-2} mol) in propane-2-ol (40 mL) was refluxed for 30 min and then cooled to room temperature with stirring. The white precipitate which appeared upon cooling was filtered off, and washed with diethyl ether. Yield: 1.8 g (86%). Anal. Calcd for $C_{11}H_{16}N_2O_2$: C, 63.4; H, 7.7; N, 13.5. Found: C, 63.0; H, 7.5; N, 13.4. ^{1}H NMR (250 MHz, 20 °C, DMSO-d_6): δ 1.19 (s, 6H, CH_3), 3.38 (s, 2H, CH_2), 6.81 (t, $J = 8$ Hz, 1H, C(5)*H*), 6.94 (d, $J = 8$ Hz, 1H, C(3)*H*), 7.37 (td, $J = 1.8$ and 8 Hz, 1H, C(4)*H*), 7.96 (dd, $J = 1.8$ and 8 Hz, 1H, C(6)*H*), 9.55 (l, 1H, N*H*). ^{13}C{^{1}H} NMR (62.896 MHz, 20 °C, DMSO-d_6): δ 27.0 (s, *C*H$_3$), 49.5 (s, *C*H$_2$), 51.4 (s, CH$_3$*C*), 117.6 (s, Ar*C*(3)H), 118.4 (s, Ar*C*), 118.7 (s, Ar*C*(5)H), 129.7 (s, Ar*C*(6)H), 132.7 (s, Ar*C*(4)H), 162.5 (s, Ar*C*(2)OH), 168.2 (s, O*C*NH). Characteristic IR absorptions (Nujol mull): 3261,1617, 1559, 1536 cm^{-1}.

L^2H_2. This ligand was prepared as L^1H_2, using phenyl salicylate (2.14 g, 1×10^{-2} mol) and 1,2-diaminopropane (0.74 g, 1×10^{-2} mol). Yield: 1.6 g (82%). Anal. Calcd for $C_{10}H_{14}N_2O_2$: C, 61.8; H, 7.3; N, 14.4. Found: C, 61.5; H, 7.1; N, 14.4. ^{1}H NMR (250 MHz, 20 °C, DMSO-d_6): δ 1.15 (d, $J = 6.5$ Hz, 3H, CH_3), 3.17 (m, 1H, CH$_3$C*H*), 3.27−3.41 (m, 2H, CH_2), 6.83 (t, $J = 8$ Hz, 1H, C(5)*H*), 6.94 (d, $J = 8$ Hz, 1H, C(3)*H*), 7.39 (td, $J = 1.0$ and 8 Hz, 1H, C(4)*H*), 7.95 (dd, $J = 1.0$ and 8 Hz, 1H, C(6)*H*), 9.55 (l, 1H, N*H*). ^{13}C{^{1}H} NMR (62.896 MHz, 20 °C, DMSO-d_6): δ 20.3 (s, *C*H$_3$), 46.4 (s, CH$_3$*C*), 46.6 (s, *C*H$_2$), 116.4 (s, Ar*C*(3)H), 117.1 (s, Ar*C*(1)), 118.3 (s, Ar*C*(5)H), 129.0 (s, Ar*C*(6)H), 133.0 (s, Ar*C*(4)H), 162.3 (s, Ar*C*(2)OH), 168.5 (s, O*C*NH). Characteristic IR absorptions (Nujol mull): 3260,1646, 1594, 1528 cm^{-1}.

L^3H_2. A mixture of phenyl salicylate (2.14 g, 1×10^{-2} mol) and 1,2-diaminoethane (0.60 g, 1×10^{-2} mol) in dichloromethane (40 mL) was stirred overnight. To the resulting white precipitate was added diethyl oxide (60 mL) and acetone (2 mL). Stirring for 3 h at room temperature yielded a bulky precipitate that was filtered off and washed with diethyl ether. Yield: 1.0 g (45%). Anal. Calcd for $C_{12}H_{16}N_2O_2$: C, 65.4; H, 7.3; N, 12.7. Found: C, 65.2; H, 7.1; N, 12.4. ^{1}H NMR (250 MHz, 20 °C, DMSO-d_6): δ 1.90 (s, 3H, CH_3), 2.04 (t, $J = 1.4$ Hz, 3H, CH_3), 3.44 (m, 2H, CH_2N), 3.60 (q, $J = 5.5$ Hz, 2H, CH_2NH), 6.98 (td, $J = 1$ and 8 Hz, 1H, C(5)*H*), 7.00 (dd, $J = 1$ and 8 Hz, 1H, C(3)*H*), 7.49 (td, $J = 1.5$ and 8 Hz,

(1) See for examples: Boyd, P. D. W.; Li, Q.; Vincent, J. B.; Folting, K.; Chang, H. R.; Streib, W. E.; Huffman, J. C.; Christou, G.; Hendrickson, D. N. *J. Am. Chem. Soc.* **1988**, *110*, 8537. McCusker, J. K.; Vincent, J. B.; Schmitt, E. A.; Mino, M. L.; Shin, K.; Coggin, A. K.; Hagen, P. M.; Huffman, J. C.; Christou, G.; Hendrickson, D. N. *J. Am. Chem. Soc.* **1991**, *113*, 3012. Delfs, C.; Gatteschi, D.; Pardi, L.; Sessoli, R.; Wieghardt, K.; Hanke, D. *Inorg. Chem.* **1993**, *32*, 3099. Goldberg, D. P.; Caneschi, A.; Delfs, C. D.; Sessoli, R.; Lippard, S. J. *J. Am. Chem. Soc.* **1995**, *117*, 5789. Sun, Z.; Gantzel, P. K.; Hendrickson, D. N. *Inorg. Chem.* **1996**, *35*, 6640. Bolcar, M. A.; Aubin, S. M. J.; Folting, K.; Hendrickson, D. N.; Christou, G. *J. Chem. Soc., Chem. Commun.* **1997**, 1485. Aromí, G.; Claude, J.-P.; Knapp, M. J.; Huffman, J. C.; Hendrickson, D. N.; Christou, G. *J. Am. Chem. Soc.* **1998**, *120*, 2977. Tsohos, A.; Dionyssopoulou, S.; Raptopoulou, C. P.; Terzis, A.; Bakalbassis, E. G.; Perlepes S. P. *Angew. Chem., Int. Ed.* **1999**, *38*, 983. Barra, A. L.; Caneschi, A.; Cornia, A.; Fabrizi de Biani, F.; Gatteschi, D.; Sangregorio, C.; Sessoli, R.; Sorace, L. *J. Am. Chem. Soc.* **1999**, *121*, 5302. Dearden, A. L.; Parsons, S.; Winpenny, R. E. P. *Angew. Chem., Int. Ed.* **2001**, *40*, 151.

(2) Aromí, G.; Aubin, S. M. J.; Bolcar, M. A.; Christou, G.; Eppley, H. J.; Folting, K.; Hendrickson, D. N.; Huffman, J. C.; Squire, R. C.; Tsai, H.-L.; Wang, S.; Wemple, M. W. *Polyhedron* **1998**, *17*, 3005. Cdiou, C.; Murrie, M.; Paulsen, C.; Villar, V.; Wernsdorfer, W.; Winpenny, R. E. P. *Chem. Commun.* **2001**, 2666. Wernsdorfer, W.; Aliaga-Alcalde, N.; Hendrickson, D. N.; Christou, G. *Nature* **2002**, *416*, 406. Gatteschi, D.; Sessoli, R. *Angew. Chem., Int. Ed.* **2003**, *42*, 268.

(3) Palopoli, C.; González-Sierra, M.; Robles, G.; Dahan, F.; Tuchagues, J.-P.; Signorella, S. *J. Chem. Soc., Dalton Trans.* **2002**, 3813 and refs. therein.

(4) Khangulov, S. V.; Pessiki, P. J.; Barynin, V. V.; Ash, D. E.; Dismukes, G. C. *Biochemistry* **1995**, *34*, 2015. Stemmler, T. L.; Sossong, T. M., Jr.; Goldstein, J. I.; Ash, D. E.; Elgren, T. E.; Kurtz, D. M., Jr.; Penner-Hahn, J. E. *Biochemistry* **1997**, *36*, 9847.

(5) Sjoeberg, B.-M. In *Structure and Bonding*; Hill, H. A. O., Sadler, P. J., Thomson, A. J., Eds.; Springer-Verlag: Berlin, 1997; Vol. 88, p 139.

(6) Cammack, R.; Chapman, A.; Lu, W.-P.; Karagouni, A.; Kelly, D. P. *FEBS Lett.* **1989**, *253*, 239.

(7) Yachandra, V. K.; DeRose, V. J.; Latimer, M. J.; Mukerjee, I.; Sauer, K.; Klein, M. P. *Science* **1993**, *260*, 675. Hoganson, C. W.; Babcock, G. *Science* **1997**, *277*, 1953. Tommos, C.; Babcock, G. *Acc. Chem. Res.* **1998**, *31*, 18. Dube, C. E.; Wright, D. W.; Pal, S.; Bonitatebus, P. J., Jr.; Armstrong, W. H. *J. Am. Chem. Soc.* **1998**, *120*, 3704. Limburg, J.; Vrettos, J. S.; Liable-Sands, L. M.; Rheingold, A. L.; Crabtree, R. H.; Brudvig, G. W. *Science* **1999**, *283*, 1524. Ruettinger, W. F.; Dismukes, G. C. *Inorg. Chem.* **2000**, *39*, 1021. Zouni, A.; Witt, H.-T.; Kern, J.; Fromme, P.; Krauss, N.; Saenger, W.; Orth, P. *Nature* **2001**, *409*, 739.

(8) (a) Gregson, A. K.; Moxon, N. T. *Inorg. Chem.* **1982**, *21*, 586. (b) Kennedy, B. J.; Murray, K. S. *Inorg. Chem.* **1985**, *24*, 1552. (c) Pecoraro, V. L.; Butler, W. M. *Acta Crystallogr.* **1986**, *C42*, 1151. (d) Kipke, C. A.; Scott, M. J.; Gohdes, J. W.; Armstrong, W. H. *Inorg. Chem.* **1990**, *29*, 2193. (e) Theil, S. Ph.D. Thesis, Université de Toulouse III, 1993. (f) Reddy, K. R.; Rajasekharan, M. V.; Tuchagues, J.-P. *Inorg. Chem.* **1998**, *37*, 5978. (g) Sailaja, S.; Reddy, K. R.; Rajasekharan, M. V.; Hureau, C.; Rivière, E.; Cano, J.; Girerd, J. J. *Inorg. Chem.* **2003**, *42*, 180.

(9) Costes, J. P.; Dahan, F. *C. R. Acad. Sci., Ser. IIc* **2001**, *4*, 97.

1H, C(4)*H*), 7.93 (dd, $J = 1.8$ and 8 Hz, 1H, C(6)*H*), 9.11 (t, $J = 5.5$ Hz, 1H, OCN*H*). $^{13}C\{^1H\}$ NMR (62.896 MHz, 20 °C, DMSO-d_6): δ 19.5 (s, *C*H$_3$), 29.8 (s, *C*H$_3$), 41.2 (s, *C*H$_2$NH), 51.0 (s, *C*H$_2$N), 116.8 (s, Ar*C*), 118.5 (s, Ar*C*(3)H), 119.2 (s, Ar*C*(5)H), 129.2 (s, Ar*C*(6)H), 134.4 (s, Ar*C*(4)H), 161.3 (s, Ar*C*(2)OH), 168.7 (s, *C*═N), 169.6 (s, O*C*NH). Characteristic IR absorptions (Nujol mull): 3383, 3350, 1644, 1600, 1577, 1539 cm^{-1}.

L^{4}H$_3$. A mixture of L^{3}H$_2$ (0.80 g, 3.6×10^{-3} mol) and salicylaldehyde (0.44 g, 3.6×10^{-3} mol) in ethanol (20 mL) was refluxed for 10 min with stirring. The solution was left to stand overnight, yielding yellow crystals that were filtered off and dried. Yield: 0.6 g (55%). Anal. Calcd for $C_{16}H_{16}N_2O_3$: C, 67.6; H, 5.7; N, 9.8. Found: C, 67.7; H, 5.3; N, 9.8. ^{1}H NMR (250 MHz, 20 °C, DMSO-d_6): δ 3.63 (q, $J = 5.5$ Hz, 2H, C*H*$_2$NH), 3.80 (t, $J = 5.5$ Hz, 2H, C*H*$_2$N), 6.88 (t + t + d, $J = 8$ Hz, 3H, C(5)*H*, C(3′)*H* and C(5′)*H*), 6.91 (d, $J = 8$ Hz, 1H, C(3)*H*), 7.32 (td, $J = 1.5$ and 8 Hz, 1H, C(4′)*H*), 7.39 (td, $J = 1.5$ and 8 Hz, 1H, C(4)*H*),7.42 (dd, $J = 1.5$ and 8 Hz, 1H, C(6′)*H*), 7.84 (dd, $J = 1.5$ and 8 Hz, 1H, C(6)*H*), 8.56 (s, 1H, *H*C═N), 9.00 (t, $J = 5.5$ Hz, 1H, OCN*H*), 12.49 (s, 1H, O*H*), 13.47 (s, 1H, O′*H*). $^{13}C\{^1H\}$ NMR (62.896 MHz, 20 °C, DMSO-d_6): δ 40.7 (s, *C*H$_2$NH), 58.4 (s, *C*H$_2$N), 116.3 (s, Ar*C*(1)), 117.3 (s, Ar*C*(3′)H), 118.2 (s, Ar*C*(3)H), 119.4 (s, Ar*C*(5)H), 119.5 (s, Ar*C*(5′)H), 119.8 (s, Ar*C*(1′)), 128.7 (s, Ar*C*(6)H), 132.6 (s, Ar*C*(6′)H), 133.2 (s, Ar*C*(4′)H), 134.5 (s, Ar*C*(4)H), 160.7 (s, Ar*C*(2)OH), 161.4 (s, Ar*C*(2′)OH), 167.8 (s, *C*═N), 169.8 (s, O*C*NH). Characteristic IR absorptions (Nujol mull): 3379,1634, 1592, 1549 cm^{-1}.

L^{5}H$_3$. A mixture of L^{1}H$_2$ (0.42 g, 2×10^{-3} mol) and salicylaldehyde (0.24 g, 2×10^{-3} mol) in propane-2-ol (10 mL) was refluxed for 10 min with stirring. The solution was set aside, yielding yellow crystals that were filtered off and dried. Yield: 0.3 g (49%). Anal. Calcd for $C_{18}H_{20}N_2O_3$: C, 69.2; H, 6.5; N, 9.0. Found: C, 68.9; H, 6.3; N, 8.8. ^{1}H NMR (250 MHz, 20 °C, DMSO-d_6): δ 1.43 (s, 6H, CH$_3$), 3.64 (d, $J = 6.2$ Hz, 2H, C*H*$_2$NH), 6.95−7.03 (m, 4H, C(5)*H*, C(3)*H*, C(3′)*H*, and C(5′)*H*), 7.43 (td, $J = 1.5$ and 8 Hz, 1H, C(4′)*H*), 7.49 (td, $J = 1.5$ and 8 Hz, 1H, C(4)*H*), 7.60 (dd, $J = 1.5$ and 8 Hz, 1H, C(6′)*H*), 7.99 (dd, $J = 1.5$ and 8 Hz, 1H, C(6)*H*), 8.70 (s, 1H, *H*C═N), 8.90 (t, $J = 6.2$ Hz, 1H, OCN*H*), 12.26 (s, 1H, O*H*), 13.96 (s, 1H, O′*H*). $^{13}C\{^1H\}$ NMR (62.896 MHz, 20 °C, DMSO-d_6): δ 26.1 (s, *C*H$_3$), 50.1 (s, *C*H$_2$-NH), 61.6 (s, *C*(CH$_3$)$_2$N), 117.4 (s, Ar*C*(1)), 117.6 (s, Ar*C*(3′)H), 118.3 (s, Ar*C*(3)H), 119.4 (s, Ar*C*(5)H), 119.8 (s, Ar*C*(5′)H), 120.0 (s, Ar*C*(1′)), 129.8 (s, Ar*C*(6)H), 133.2 (s, Ar*C*(6′)H), 133.3 (s, Ar*C*(4′)H), 134.5 (s, Ar*C*(4)H), 160.1 (s, Ar*C*(2)OH), 162.0 (s, Ar*C*(2′)OH), 163.8 (s, *C*═N), 169.4 (s, O*C*NH). Characteristic IR absorptions (Nujol mull): 3380, 1644, 1630, 1597, 1544 cm^{-1}.

L^{6}H$_3$. A mixture of L^{2}H$_2$ (0.19 g, 1×10^{-3} mol) and salicylaldehyde (0.12 g, 1×10^{-3} mol) in dichloromethane (10 mL) was refluxed for 10 min with stirring. The solution was concentrated and cooled. Addition of pentane yielded a yellow sticky product that was washed with pentane and dried. Yield: 0.1 g (36%). Anal. Calcd for $C_{17}H_{18}N_2O_3$: C, 68.4; H, 6.1; N, 9.4. Found: C, 68.0; H, 5.8; N, 9.3. ^{1}H NMR (250 MHz, 20 °C, DMSO-d_6): δ 1.39 (d, $J = 6.5$ Hz, 3H, CH$_3$), 3.54 and 3.67 (m, 2H, C*H*$_2$NH), 3.80 (m, 1H, CH$_3$C*H*N), 6.97−7.00 (m, 4H, C(5)*H*, C(3)*H*, C(3′)*H*, and C(5′)-*H*), 7.43 (td, $J = 1.5$ and 8 Hz, 1H, C(4′)*H*), 7.50 (t, $J = 8$ Hz, 1H, C(4)*H*), 7.52 (dd, $J = 1.5$ and 8 Hz, 1H, C(6′)*H*), 7.93 (dd, $J = 1.5$ and 8 Hz, 1H, C(6)*H*), 8.65 (s, 1H, *H*C═N), 9.01 (t, $J = 6.5$ Hz, 1H, OCN*H*), 12.45 (s, 1H, O*H*), 13.41 (s, 1H, O′*H*). $^{13}C\{^1H\}$ NMR (62.896 MHz, 20 °C, DMSO-d_6): δ 20.0 (s, *C*H$_3$), 45.4 (s, *C*H$_2$NH), 63.0 (s, CH$_3$*C*HN), 115.6 (s, Ar*C*(1)), 116.5 (s, Ar*C*(3′)H), 117.4 (s, Ar*C*(3)H), 118.7 (s, Ar*C*(5)H), 118.7 (s, Ar*C*(5′)H), 118.8 (s, Ar*C*(1′)), 128.1 (s, Ar*C*(6)H), 131.8 (s, Ar*C*(6′)H), 132.4 (s, Ar*C*(4′)H), 133.7 (s, Ar*C*(4)H), 159.9 (s, Ar*C*(2)OH), 160.6 (s, Ar*C*(2′)OH), 165.2 (s, *C*═N), 169.0 (s, O*C*NH). Characteristic IR absorptions (Nujol mull): 3364, 1645, 1633, 1593, 1544 cm^{-1}.

Mn^{III} Complexes. [L^{6}Mn(CH$_3$OH)$_2$] (1). A mixture of L^{2}H$_2$ (0.40 g, 2×10^{-3} mol) and salicylaldehyde (0.24 g, 2×10^{-3} mol) in methanol (20 mL) was heated for 30 min and then left to cool under stirring. NaOH (0.24 g, 6×10^{-3} mol) was first added and then Mn(OAc)$_2$·4H$_2$O (0.5 g, 2×10^{-3} mol). The solution which turned darker immediately was stirred for 2 h and set aside; crystals appeared 2 days later. Yield: 0.42 g (51%). Anal. Calcd for $C_{19}H_{23}MnN_2O_5$: C, 55.1; H, 5.6; N, 6.8. Found: C, 54.7; H, 5.3; N, 6.8.

[L$^5_4$Mn$_4$(H$_2$O)$_2$](CH$_3$OH)$_2$ (2). A mixture of L^{1}H$_2$ (0.75 g, 3.6×10^{-3} mol) and salicylaldehyde (0.44 g, 3.6×10^{-3} mol) in methanol (20 mL) was heated for 30 min and then left to cool under stirring. NaOH (0.43 g, 1.08 10^{-2} mol) was first added and then Mn(OAc)$_2$·4H$_2$O (0.95 g, 3.6×10^{-3} mol). The solution which turned darker immediately was stirred for 2 h and set aside; crystals appeared 2 days later. Yield: 0.40 g (29%). Anal. Calcd for $C_{74}H_{80}Mn_4N_8O_{16}$: C, 57.1; H, 5.2; N, 7.2. Found: C, 56.8; H, 5.1; N, 6.9.

[L^{4}Mn(CH$_3$OH)]$_n$ (3). To a solution of L^{4}H$_2$ (0.30 g, 1.1×10^{-3} mol) in methanol (20 mL) was first added NaOH (0.13 g, 3.3×10^{-3} mol) and then Mn(OAc)$_2$·4H$_2$O (0.27 g, 1.1×10^{-3} mol). The reaction mixture was heated for 30 min and then left to cool under stirring. NaOH (0.24 g, 6×10^{-3} mol) was first added and then Mn(OAc)$_2$·4H$_2$O (0.5 g, 2×10^{-3} mol). The solution which turned darker immediately was stirred for 2 h and set aside; crystals appeared 3 days later. Yield: 0.16 g (40%). Anal. Calcd for $C_{17}H_{17}MnN_2O_4$: C, 55.4; H, 4.6; N, 7.6. Found: C, 55.1; H, 4.5; N, 7.4.

Crystallographic Data Collection and Structure Determination for 1, 2, and 3. Crystals suitable for X-ray analyses were obtained by slow evaporation of the corresponding methanol solutions. The selected crystal of **1** (red plate, $0.35 \times 0.20 \times 0.15$ mm^3) was mounted on an Oxford-Diffraction Xcalibur diffractometer using a graphite-monochromated Mo Kα radiation ($\lambda = 0.71073$ Å) and equipped with an Oxford Instruments Cryojet cooler device. Data were collected[10] at 190 K with 4 runs ($\varphi = 0°$, 90°, 180°, 270°) and ω scans up to $\theta = 30.3°$ (153 frames with a maximum time of 50 s). The selected crystal of **2** (dark-red plate, $0.30 \times 0.15 \times 0.10$ mm^3) was mounted on a Stoe imaging plate diffractometer system (IPDS) using a graphite monochromator ($\lambda = 0.71073$ Å), and equipped with an Oxford Cryosystems cooler device. Data were collected[11] at 180 K with a φ oscillation movement ($\varphi = 0.0-200.2°$, $\Delta f = 1.1°$), the crystal-to-detector distance being equal to 80 mm (max θ value 24.2°). The selected crystal of **3** (red plate, $0.35 \times 0.30 \times 0.15$ mm^3) was mounted on an Oxford-Diffraction Xcalibur diffractometer using a graphite-monochromated Mo Kα radiation ($\lambda = 0.71073$ Å) and equipped with an Oxford Instruments Cryojet cooler device. Data were collected[10] at 180 K with 4 runs ($\varphi = 0°$, 90°; 180°, 270°) and ω scans up to $\theta = 30.3°$ (164 frames with a maximum time of 40 s). There were 8333 reflections collected for **1**, of which 5041 were independent ($R_{int} = 0.0408$). Gaussian absorption corrections[12] were applied ($T_{min-max} = 0.5631-0.6758$). There were 34187 reflections collected for **2**, of which 5560 were independent ($R_{int} = 0.0673$). Numerical absorption corrections[13] were applied ($T_{min-max} = 0.4555-0.5826$). There were 12206 reflections collected for **3**, of

(10) *CRYSALIS*, version 169; Oxford-Diffraction, Poland, 2001.
(11) *STOE, IPDS Manual*, version 2.93; Stoe & Cie: Darmstadt, Germany, 1997.
(12) Spek, A. L. *PLATON*. An Integrated Tool for the Analysis of the Results of a Single-Crystal Structure Determination. *Acta Crystallogr.* **1990**, *A46*, C34.
(13) *X-SHAPE. Crystal Optimisation for Numerical Absorption Corrections*, revision 1.01; Stoe & Cie: Darmstadt, Germany, 1996.

Table 1. Crystallographic Data for Complexes **1**, **2**, and **3**

	1	**2**	**3**
chem formula	$C_{19}H_{23}MnN_2O_5$	$C_{37}H_{40}Mn_2N_4O_8$	$C_{17}H_{17}MnN_2O_4$
fw	414.33	778.61	368.27
space group	$P\bar{1}$	*Pbcn* (No. 60)	$P2_1/c$
a, Å	7.8582(14)	23.8283(15)	11.7443(14)
b, Å	10.9225(16)	11.1605(7)	7.5996(10)
c, Å	12.4882(18)	26.152(2)	18.029(2)
α, deg	67.231(14)		
β, deg	72.134(14)		100.604(10)
γ, deg	82.589(13)		
V, Å^{-3}	940.6(3)	6954.8(8)	1581.6(3)
Z	2	8	4
ρ_{calcd}, g cm^{-3}	1.463	1.487	1.547
λ, Å	0.71073	0.71073	0.71073
T, K	190	180	180
μ(Mo Kα), cm^{-1}	7.35	7.86	8.59
R^a obsd, all	0.0371, 0.0597	0.0453, 0.0593	0.0296, 0.0351
$R_w{}^b$ obsd, all	0.0606, 0.0704	0.0960, 0.1014	0.0559, 0.0585

^{a} $R = \sum||F_o| - |F_c||/\sum|F_o|$. ^{b} $R_w = [\sum w(|F_o^2| - |F_c^2|)^2/\sum w|F_o^2|^2]^{1/2}$.

Table 2. Selected Bond Lengths and Angles for Complexes **1**, **2**, and **3**

	1	**2** Mn six-coordinate	**2** Mn five-coordinate	**3**
Mn−$O_{phenol(amide)}$	1.857(1)	1.852(3)	1.839(3)	1.856(1)
Mn−$O_{phenol(imine)}$	1.897(1)	1.879(3)	1.878(2)	1.918(1)
Mn−$N_{(amide)}$	1.960(2)	1.937(3)	1.905(3)	1.955(1)
Mn−$N_{(imine)}$	2.005(2)	1.990(3)	1.983(3)	1.990(1)
Mn−$O_{(amide)}$		2.255(2)	2.074(3)	2.219(1)
Mn−$OHCH_3$	2.264(2) 2.290(1)			2.316(1)
Mn−OH_2		2.352(3)		
O=$C_{(amide)}$	1.276(2)	1.267(4)	1.266(4)	1.272(2)
Mn···$Mn_{shortest}$	6.8800(6)	5.9712(7)	5.9712(7)	5.1733(4)

which 4438 were independent ($R_{int} = 0.0471$). Gaussian absorption corrections[12] were applied ($T_{min-max} = 0.55373-0.6820$).

The structures were solved using SHELXS-97[14] and refined on F^2 by full-matrix least-squares using SHELXL-97[15] with anisotropic displacement parameters for all non-hydrogen atoms. H atoms were introduced in calculations using the riding model, except those bonded to the O(3) and O(4) atoms in **1** and to the O(7) atom in **2** that were allowed to vary. Isotropic U_H values were 1.1 times higher than those of the atom to which they are bonded. The atomic scattering factors and anomalous dispersion terms were taken from the standard compilation.[16] The maximum and minimum peaks on the final difference Fourier map were 0.271 and −0.284 e Å^{-3} for **1**, 0.323 and −0.319 e Å^{-3} for **2**, and 0.306 and −0.308 e Å^{-3} for **3**. Drawings of the molecules were performed with the program ZORTEP.[17] Crystal data collection and refinement parameters are given in Table 1, and selected bond distances and angles are gathered in Table 2.

Physical Measurements. Elemental analyses were carried out at the Laboratoire de Chimie de Coordination Microanalytical Laboratory in Toulouse, France, for C, H, and N. IR spectra were recorded on a GX system 2000 Perkin-Elmer spectrophotometer. Samples were run as KBr pellets. 1D ^{1}H NMR spectra were acquired at 250.13 MHz on a Bruker WM250 spectrometer. 1D ^{13}C spectra using ^{1}H broadband decoupling {^{1}H}^{13}C and gated ^{1}H decoupling with selective proton irradiation were obtained with a Bruker WM250 facility working at 62.89 MHz. 2D ^{1}H COSY experiments using standard programs and 2D pulse-field gradient HMQC ^{1}H−^{13}C correlation using a PFG-HMQC standard program were performed on a Bruker AMX400 spectrometer. Chemical shifts are given in ppm versus TMS (^{1}H and ^{13}C) using $(CD_3)_2SO$ as solvent. Magnetic data were obtained with a Quantum Design MPMS SQUID susceptometer. All samples were 3 mm diameter pellets molded from ground crystalline samples. Magnetic susceptibility measurements were performed in the 2−300 K temperature range in a 0.5 T applied magnetic field, and diamagnetic corrections were applied by using Pascal's constants.[18] Isothermal magnetization measurements were performed up to 5 T at 2 K. The magnetic susceptibility has been computed by exact calculation of the energy levels associated to the spin Hamiltonian through diagonalization of the full matrix with a general program for axial symmetry,[19] and with the MAGPACK program package[20] in the case of magnetization. Least-squares fittings were accomplished with an adapted version of the function-minimization program MINUIT.[21]

Results and Discussion

Syntheses. The ligands L^4H_3, L^5H_3, and L^6H_3 used in this study for manganese complexation have been prepared according to an experimental procedure adapted from an earlier described method.[9] Owing to the involvement of one amide and one imine linkages, these ligands include an uncommon asymmetrical trianionic tetradentate N_2O_2 coordination site with one amide, one imine, and two phenol functions. Accordingly, their synthesis requires a stepwise process: the amide part of the ligands has been synthesized by the method described earlier by Daidone.[22] Reaction of phenyl salicylate with 1,2-diamino-2-methylpropane or 1,2-diaminopropane in propane-2-ol is straightforward and produces the pure half-unit ligands L^1H_2 and L^2H_2 in good yields (Scheme 1). "Half-unit" is meant to indicate that only one function of the diamine reactant has been involved in the reaction process.[23] When similar reaction conditions are used with 1,2-diaminoethane, a mixture of the half-unit and of the symmetrical ligands is obtained (see Scheme 2). Use of dichloromethane as solvent without heating produces the half-unit in higher yield. After 12 h and after dichloromethane removal, diethyl ether including a small amount of acetone was added to the resulting pasty product. Stirring induces formation of a bulky white precipitate which is easily isolated by filtration. Spectroscopic analyses (NMR, IR) confirm the presence of an L^3H_2 derivative in which a Schiff base condensation has occurred between the unreacted amine function of the half-unit and acetone (Scheme 2). Further

(14) Sheldrick, G. M. *SHELXS-97. Program for Crystal Structure Solution*; University of Göttingen: Göttingen, Germany, 1990.
(15) Sheldrick, G. M. *SHELXL-97. Program for the refinement of crystal structures from diffraction data*; University of Göttingen: Göttingen, Germany, 1997.
(16) *International Tables for Crystallography*; Kluwer Academic Publishers: Dordrecht, The Netherlands, 1992; Vol. C.
(17) Zsolnai, L.; Pritzkow, H.; Huttner, G. *ZORTEP. Ortep for PC, Program for Molecular Graphics*; University of Heidelberg: Heidelberg, Germany, 1996.
(18) Pascal, P. *Ann. Chim. Phys.* **1910**, *19*, 5.
(19) Clemente-Juan, J. M.; Mackiewicz, C.; Verelst, M.; Dahan, F.; Bousseksou, A.; Sanakis, Y.; Tuchagues, J.-P. *Inorg. Chem.* **2002**, *41*, 1478.
(20) (a) Borrás-Almenar, J. J.; Clemente-Juan, J. M.; Coronado, E.; Tsukerblat, B. S. *Inorg. Chem.* **1999**, *38*, 6081. (b) Borrás-Almenar, J. J.; Clemente-Juan, J. M.; Coronado, E.; Tsukerblat, B. S. *J. Comput. Chem.* **2001**, *22*, 985−991.
(21) James, F.; Roos, M. *MINUIT Program*, a System for Function Minimization and Analysis of the Parameters Errors and Correlations. *Comput. Phys. Commun.* **1975**, *10*, 345.
(22) Daidone, G.; Raffa, D.; Maggio, B.; Plescia, S.; Matera, M.; Caruso, A. *Farmaco, Ed. Sci.* **1990**, *45*, 285.
(23) Costes, J. P.; Fenton, D. E. *J. Chem. Soc., Dalton Trans.* **1983**, 2235.

Scheme 1

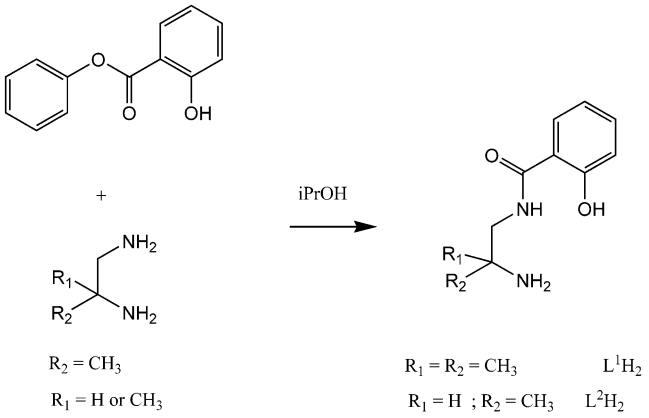

Scheme 2

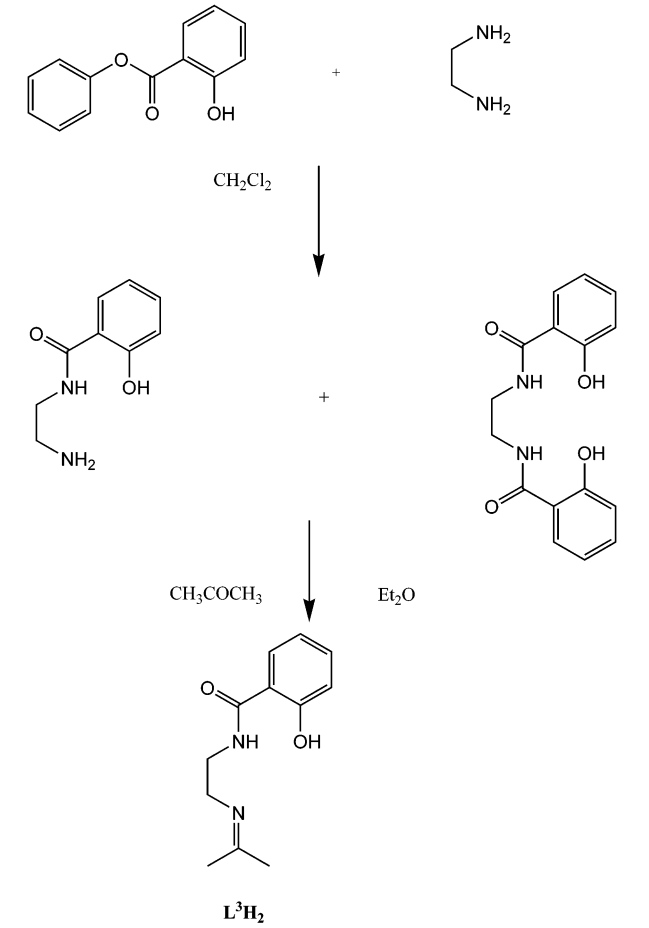

reaction of the L^1H_2, L^2H_2, and L^3H_2 half-unit ligands with salicylaldehyde yields L^5H_3, L^6H_3, and L^4H_3, respectively. These new asymmetrical ligands possess an inner tetradentate N_2O_2 coordination site and an outer amido oxygen donor atom (Scheme 3). The complexes are readily obtained by aerobic reaction of the preformed polyfunctional ligand or the ligand prepared in situ with manganese(II) acetate in methanol in the presence of sodium hydroxide. Within 2−3 days, the desired complexes were obtained as crystals from the resulting reaction media with satisfying yields.

IR and NMR Data. Considering that the original half-unit ligands L^1H_2, L^2H_2, and L^3H_2 are the cornerstone of the

Scheme 3

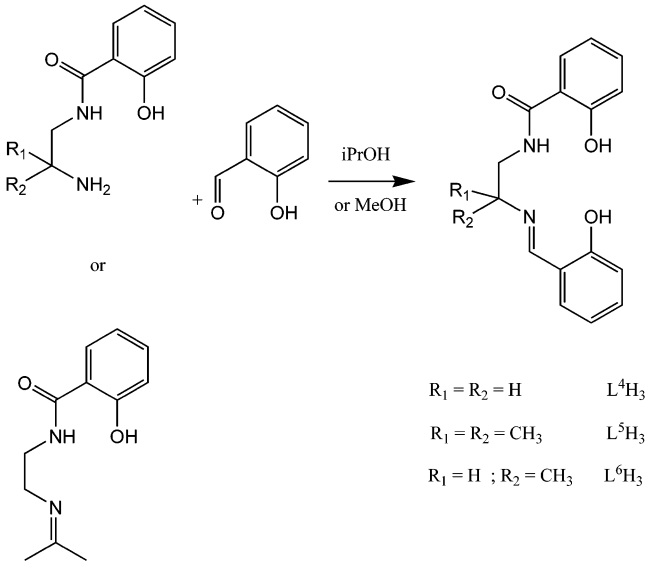

process, their spectroscopic parameters have been investigated. Surprisingly, the characteristic sharp NH stretching of the amide function is broadened and lowered in the infrared spectra (Nujol mulls) of L^1H_2 and L^2H_2, implying that the NH group is involved in a strong hydrogen bond.[24] On the contrary, two sharp absorptions are present in the IR spectra of L^3H_2 at 3383 and 3350 cm^{-1}. As a consequence, the C═O stretch is also lowered in the L^1H_2 ligand (1617 cm^{-1}) while it appears at 1644 cm^{-1} for L^3H_2 and L^4H_3. NMR results, obtained in DMSO solutions, confirm this behavior, with a sharp triplet for the amide HN proton at 9.11 ppm resulting from its coupling with the neighboring methylene group in the case of L^3H_2, L^4H_3, and L^5H_3, while broad signals are observed at 9.55 ppm for L^1H_2 and L^2H_2. Unique NH stretching bands are also present in the infrared spectra of L^4H_3 and L^5H_3 (3380 cm^{-1}). Amide II bands are not easily assigned, due to presence of C═C and imine C═N bands in the same spectral zone.

In order to complete the characterization of the complexes, we have performed a detailed study of the ^1H and ^{13}C NMR spectra of the L^5H_3 ligand. $^1H-^{13}C$ HMQC-GS, HMQC-LR, and $^1H-^1H$ COSY experiments allowed us to assign the whole sets of ^1H and ^{13}C signals. Eventually, IR and NMR data do confirm the structure of these asymmetrical polydentate ligands.

Molecular Structure of $[L^6Mn(CH_3OH)_2]$, 1, $[L^5{}_4Mn_4(H_2O)_2](CH_3OH)_2$, 2, and $[L^4Mn(CH_3OH)]_n$, 3. ZORTEP views of the molecular structure of the manganese(III) complexes **1**−**3** are sketched in Figures 1−3, respectively. Relevant bond distances and angles are gathered in Table 2.

The racemic 1,2-diaminopropane used to prepare L^2H_2 may yield both geometrical and optical isomers. The NMR study of L^2H_2 clearly demonstrates that the geometrical isomer where the methyl substituent is remote from the amide function is the only one obtained. Furthermore, the achiral $P\bar{1}$ space group of complex **1** requires the presence of both

(24) Silverstein, R. M.; Webster, F. W. *Spectrometric Identification of Organic Compounds*, 6th Ed.; John Wiley: New York, 1975.

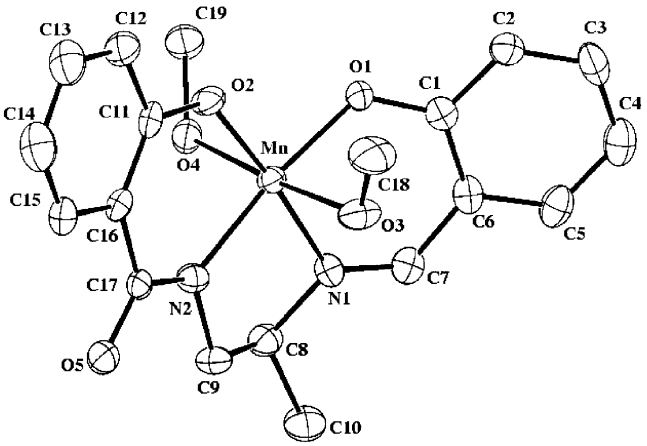

Figure 1. Molecular plot for **1** with ellipsoids drawn at the 50% probability level.

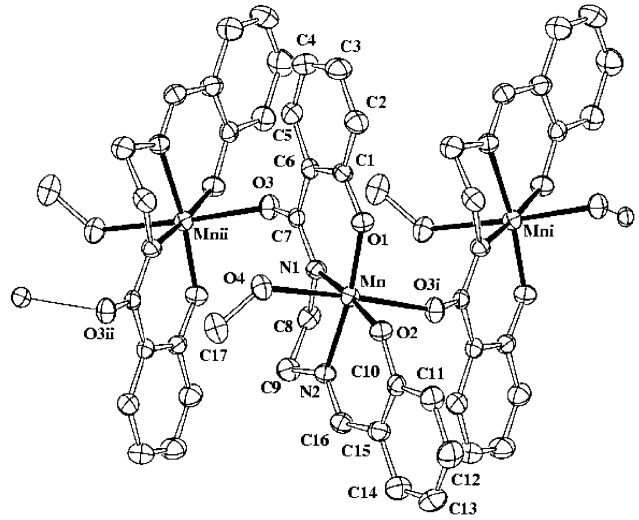

Figure 2. Molecular plot for **3** with ellipsoïds drawn at the 50% probability level. Symmetry operations: i, $1 - x$, $^1/_2 + y$, $^1/_2 - z$; ii, $1 - x$, $-^1/_2 + y$, $^1/_2 - z$.

enantiomers in the unit cell. The Mn^{III} ion of complex **1** is coordinated to the amido and imine nitrogen and the two phenoxo oxygen atoms while the amide oxygen atom is not involved in coordination (Figure 1). The four donor atoms of the ligand form the equatorial plane of a distorted octahedron around manganese, while the apical positions are occupied by the oxygen atom of two methanol molecules. The axial Mn−O bonds (2.264(2) and 2.290(1) Å) are longer than the basal ones: 1.857(1) and 1.897(1) Å for Mn−O, and 1.960(2) and 2.005(2) Å for Mn−N. The central Mn−N−C−C−N five-membered ring is not planar and has a δ conformation for the *S* enantiomer; by symmetry, the *R* enantiomer has a λ conformation: the methyl substituent of both enantiomers is thus in an equatorial position. The equatorial N_2O_2 donor atoms are not strictly coplanar, but alternately displaced by 0.05 Å from the mean Mn, O1, N1, N2, O2 plane. Both phenyl rings deviate from this mean plane in such a way that the complex molecule displays a boat-shaped conformation. The neutral molecules of **1** are linked together by two hydrogen bonds involving the axial MeOH molecules and the amide oxygen atoms. Due to their head to tail arrangement, the amido oxygen atoms are

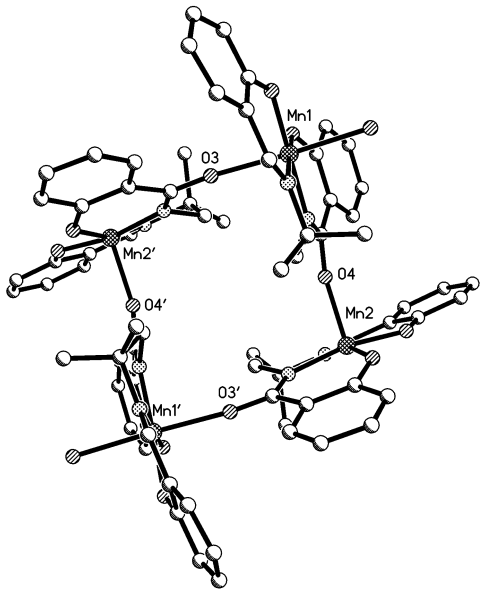

Figure 3. Structure of the tetranuclear unit of complex **2**. Symmetry operation: ′, $1 - x$, y, $^1/_2 - z$.

hydrogen-bonded to two different MeOH molecules coordinated to the previous and next manganese centers. This arrangement creates an infinite ribbon with two slightly different Mn···Mn distances (6.8880(6) and 6.9615(6) Å). Furthermore, $\pi-\pi$ stackings involving the phenyl rings of the salicylaldimine part of the ligand operate between the ribbons. Alternation of these stacked cycles yields a two-dimensional arrangement of the neutral complex molecules running parallel to the *c* axis, with a Mn···Mn separation of 7.3790(6) Å (Figure S1).

The structures of complexes **2** and **3** are significantly different from that of complex **1**: their amido oxygen atoms are involved in the coordination process as well as the related nitrogen atom, allowing the amido function to actually bridge adjacent manganese(III) ions, thus leading to polynuclear structures. In both cases, the bridge is constituted by an equatorial N_{amido} donor and its related O_{amido} as axial donor to the adjacent Mn^{III} ion.

The actual structure of $[L^4Mn(CH_3OH)]_n$, **3**, is an infinite zigzag chain of six-coordinated Mn^{III} ions (Figure 2). As in the previous complex **1**, the N_2O_2 donor set of the asymmetrical ligand constitutes the equatorial coordination plane while the apical positions of the octahedron are occupied by oxygen atoms from a solvent molecule (methanol) and from the amido function of a neighboring complex molecule. The Mn^{III} ion is slightly displaced from the mean equatorial plane (0.05 Å) toward the methanol molecule although the Mn−O_{amido} bond is shorter (2.219(1) Å) than the Mn−$O_{methanol}$ one (2.316(1) Å). The central Mn−N−C−C−N five-membered ring is not planar and has a λ gauche conformation. As a whole, the ligand is less distorted than in **1**, with only one phenyl ring deviating from the N_2O_2 equatorial coordination plane. The L^4Mn constituting units are organized into infinite zigzag chains with a head to tail arrangement allowing coordination of the amido oxygen of each unit to the metal ion of the next unit in the chain. In a zigzag chain, two arrays of parallel molecules may be

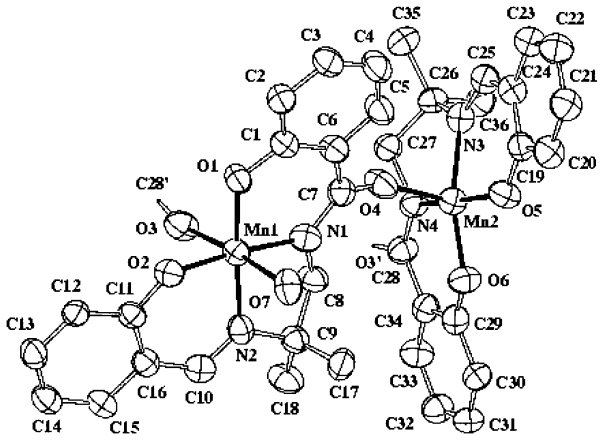

Figure 4. ZORTEP plot of the asymmetric unit for **2** with ellipsoids drawn at the 50% probability level.

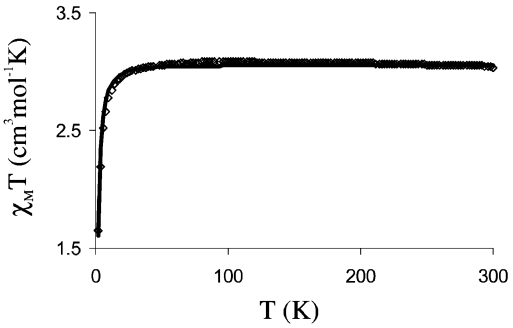

Figure 5. Thermal dependence of $\chi_M T$ for **1** at 0.1 T. The full line (—) corresponds to the best data fit.

distinguished: starting from a molecule ranked number *n*, the molecules ranked *n*, *n* + 2, *n* + 4, and so forth, are parallel to each other while the molecules *n* + 1, *n* + 3, and so forth, form a second array of parallel molecules. The angle between the two arrays is equal to 38.2°.

In complex **2**, $[L^5{}_4Mn_4(H_2O)_2](CH_3OH)_2$, four Mn^{III} ions are linked together by four amido groups to form a parallelogram shaped tetranuclear species (Figure 3) composed of two asymmetric units, each one including one L^5-Mn and one $L^5Mn(H_2O)$ constituting units as shown in Figure 4. As a result, the coordination of the two metal ions is different: Mn1 is six-coordinate while Mn2 is five-coordinate. The apical positions of the Mn1 coordination octahedron are occupied by the amido oxygen and a water molecule while the N_2O_2 equatorial donor set from L^5 is strictly planar, the Mn^{III} deviation from this plane being negligible (0.0100(5) Å). The apical position of the Mn2 square-pyramidal coordination is occupied by an amido oxygen atom. The four basal N_2O_2 donor atoms deviate from the mean coordination plane by less than 0.06 Å while Mn2 and the amido oxygen atom are displaced in the same direction by 0.1921(4) and 2.554(3) Å, respectively. The Mn2−O4 apical bond length (2.074(3) Å) is slightly larger than the equatorial Mn−O bonds (Mn2−O5 = 1.878(2) and Mn2−O6 = 1.839(3) Å). A larger difference (ca. 0.44 Å) is observed for the Mn1−O bonds. Furthermore, the Mn1−O_{amido} bond is significantly longer than the related Mn2−O bond. The dimethyl group of the diamino chain is remote from the amido function. The central Mn−N−C−C−N five-membered ring is not planar with a λ gauche conformation for the five-coordinate Mn2, and a δ conformation for the six-coordinate Mn1. The edges of the parallelogram shaped tetranuclear species equal 5.971(2) and 6.149(2) Å while its diagonals equal 7.529(3) and 8.638(3) Å. The shortest metal−metal intercluster contact of 6.747(1) Å precludes significant intermolecular magnetic interactions. A methanol molecule, not involved in coordination, is hydrogen bonded to the water molecule coordinated to the octahedral Mn^{III} ion and to the phenoxo oxygen atom linked to the five-coordinate Mn^{III} ion.

It is worth noticing that in the three complexes the bond lengths are in the same increasing order: Mn−O(phenoxo of the amido moiety) < Mn−O(phenoxo of the imine moiety) < Mn−N_{amido} < Mn−N_{imine} < Mn−O_{amido} < Mn−O(MeOH) < Mn−O(H_2O).

Magnetic Properties. The magnetic susceptibility of complexes **1**, **2**, and **3** has been measured in the 2−300 K temperature range in a 0.5 T applied magnetic field. The magnetic behavior of complex **1** is shown in Figure 5 as the thermal variation of the $\chi_M T$ versus *T* plot. χ_M is the molar magnetic susceptibility corrected for the diamagnetism of the ligands.[18] The $\chi_M T$ product is practically constant in the 300−50 K range with an observed value (3.05 ± 0.03 cm^3 K mol^{-1}) corresponding to an isolated high-spin Mn^{III} ion. On further lowering the temperature, $\chi_M T$ decreases down to 1.66 cm^3 K mol^{-1} at 2 K. The molecular structure of **1** shows that the metal centers are linked by hydrogen bonds and $\pi-\pi$ stacking, and it is known that such interactions are able to transmit magnetic interactions.[25] As the $\pi-\pi$ stackings are located in the equatorial plane of the Mn centers, their effect may be anticipated to be predominant. From a magnetic point of view, the two-dimensional arrangement of complex **1** may then be reduced to a dinuclear one. The experimental magnetic data may then be analyzed on the basis of the spin Hamiltonian $H = -2JS_{Mn1}S_{Mn2} + DS_z{}^2{}_{Mn}$, where *D* is the axial single-ion zero field splitting (ZFS). The best fit yields an interaction parameter equal to − 0.2 cm^{-1} with $g = 2.03$, $D = -0.01$ cm^{-1}, and an agreement factor R ($=\Sigma[(\chi T)_{obsd} - (\chi T)_{calcd}]^2/\Sigma[(\chi T)_{obsd}]^2$) of 3×10^{-5}. However, almost equally good fits may be obtained for *D* values ranging from 3 to −3 cm^{-1}. This indetermination of the axial single-ion ZFS of Mn^{III} was confirmed by an error-surface plot showing that while the value of *J* is well determined by the fitting procedure, the value of *D* is not.

The magnetic data obtained for complex **3** are shown in Figure 6. At 300 K, the $\chi_M T$ product, 3.07 cm^3 K mol^{-1}, corresponds to the value expected for an isolated high-spin Mn^{III} ion. It decreases very smoothly down to 2.93 cm^3 K mol^{-1} at 150 K and then more steeply, reaching 1.27 cm^3 K mol^{-1} at 10 K. Further temperature decrease results in a sharp $\chi_M T$ increase with a maximum of 2.08 cm^3 K mol^{-1}at 5 K,

(25) Colacio, E.; Costes J.-P.; Kivekas, R.; Laurent, J.-P.; Ruiz, J.; Sundberg, M. *Inorg. Chem.* **2002**, *41*, 1478. Vazquez, M.; Taglietti, A.; Gatteschi, D.; Sorace, L.; Sangregorio, C.; Gonzalez, A. M.; Maneiro, M.; Pedrido, R. M.; Bermejo, M. R. *Chem. Commun.* **2003**, 1840.

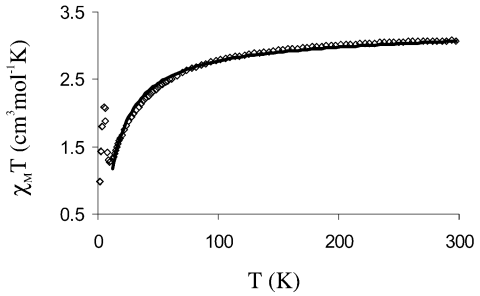

Figure 6. Thermal dependence of $\chi_M T$ for **3** at 0.1 T. The full line (—) corresponds to the best data fit.

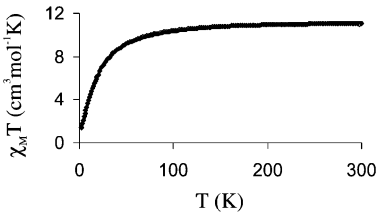

Figure 7. Thermal dependence of $\chi_M T$ for **2** at 0.1 T. The full line (—) corresponds to the best data fit.

followed by a steep decrease down to 0.99 cm^3 K mol^{-1} at 2 K. For an infinite chain of $^4/_2$ local spins, the simpler analytical expression that may be used to fit the experimental data derives from Fisher's expression:[26]

$$\chi T = [Ng^2\beta^2 S(S+1)/3k][(1+u)/(1-u)] \text{ with}$$
$$u = \coth[-2JS(S+1)/kT] - [kT/-2JS(S+1)]$$

The best agreement between experimental and calculated data from 300 to 20 K corresponds to $J = -1.1$ cm^{-1} and $g = 2.05$ with an agreement factor R ($=\sum[(\chi T)_{obsd} - (\chi T)_{calcd}]^2/\sum[(\chi T)_{obsd}]^2$) of 3.6×10^{-4}. It is not possible to fit the experimental data in the low-temperature range (20−2 K). Indeed, the sharp increase is reminiscent of a magnetic phase transition triggered by a 3D ordering, or a spin canting phenomenon. In complex **3**, the 38.2° angle between the two arrays of parallel spins (see molecular structure section) clearly indicates that spin canting is most probably responsible for the magnetic phase transition at low temperature. Magnetization studies at 2 K show the presence of an hysteresis loop with a small coercive field (260 G) and a remnant magnetization of 0.24 $N\beta$ (Figure S2 in Supporting Information). As expected for spin canting, the saturation magnetization (1.84 $N\beta$) does not reach the $4N\beta$ value of high-spin Mn^{III}.

The magnetic data obtained for complex **2** are shown in Figure 7. The $\chi_M T$ product decreases smoothly from 11.02 cm^3 K mol^{-1} at 300 K, down to 9.20 cm^3 K mol^{-1} at 50 K, and then more abruptly down to 1.41 cm^3 K mol^{-1} at 2 K. An initial fit (not shown) was performed by considering the simplifying assumption that the four magnetically interacting Mn^{III} ions are at the vertices of a square (unique J parameter). A good agreement ($R = 2 \times 10^{-4}$) with the experimental data was obtained for the following parameter values: $J = -1.2$ cm^{-1}, $g = 1.93$, par (paramagnetic impurity) = 5.6% (D fixed to 0 cm^{-1}). With the high value obtained for par seeming unreasonable in view of the quality of the microcrystalline sample, we then considered a model involving one J parameter and two D terms. Indeed, considering their ligand environment, the four Mn centers of the tetranuclear complex **2** cannot have the same axial single-ion ZFS parameter: in the following, D_1 is related to the six-coordinate Mn centers and D_2 to the five-coordinate Mn centers. The best fit ($R = 1 \times 10^{-4}$) was obtained for the following parameter values: $J = -1.1$ cm^{-1}, $D_1 = 2.2$ cm^{-1}, $D_2 = -2.8$ cm^{-1}, $g = 1.97$. Extensive calculations were then carried out in order to draw several error-surface plots: the D versus J error-surfaces showed that the value of J is unique and well determined by the fitting procedure; the D_2 versus D_1 error-surfaces showed two symmetry-related minima corresponding, as expected, to the $D_1 \leftrightarrow D_2$ permutation. The $D_1 = 2.2$ cm^{-1}, $D_2 = -2.8$ cm^{-1} couple may be considered as having more physical meaning than its $D_1 = -2.8$ cm^{-1}, $D_2 = 2.2$ cm^{-1} counterpart: the square pyramidal ligand environment of Mn2 (Mn2′) may be considered as yielding larger axial elongation than the axially elongated octahedral ligand environment of Mn1 (Mn1′). The obtained D values are in the range of those previously reported.[8e,27] Positive D parameters are usually associated with either tetragonal compression or trigonal bipyramidal five-coordination.[27a,28] However, by considering the interaction between the ground state and LMCT states with the valence bond configuration interaction (VBCI) model, it has been recently shown that D can be positive for tetragonally elongated Mn^{III} complexes.[29]

Conclusion

Trianionic asymmetrical ligands with amide and imine functions have been first used to prepare Cu−Gd complexes, with the aim to promote self-assembly of dinuclear units in order to obtain new polynuclear systems with a large ground spin-state.[9,30] Our preparative conditions differ from the synthetic process recently described, where the so-called "intermediate product" (corresponding to the half-unit) was not characterized.[30] From a synthetic point of view, the most striking result originates from the presence or absence of one or two methyl substituents at the remote position of the diamino fragment in these asymmetrical polydentate ligands, which allows an impressive variation in the nuclearity of the manganese complexes. Indeed, it is possible to isolate a mononuclear complex (**1**), a tetranuclear one (**2**), or a 1D chain (**3**) when one (L^6H_3), two (L^5H_3), or no (L^4H_3) methyl substituents are located away from the N_2O_2 coordination site, respectively. Another interesting property of these Mn^{III}

(26) Fisher, M. E. *Am. J. Phys.* **1964**, *32*, 343.

(27) (a) Kennedy, B. J.; Murray, K. S. *Inorg. Chem.* **1985**, *24*, 1557. (b) Wieghardt, K. *Angew. Chem., Int. Ed. Engl.* **1989**, *28*, 1153. (c) Thorp, H. H.; Brudvig, G. W. *New J. Chem.* **1991**, *15*, 479. (d) Zhang, Z.; Brouca-Cabarrecq, C.; Hemmert, C.; Dahan, F.; Tuchagues, J. P. *J. Chem. Soc., Dalton Trans.* **1995**, 1453.

(28) Whittaker, J. W.; Whittaker, M. M. *J. Am. Chem. Soc.* **1991**, *113*, 5528.

(29) Mossin, S.; Weihe, H.; Barra, A. L. *J. Am. Chem. Soc.* **2002**, *124*, 8764.

(30) (a) Kido, T.; Nagasato, S.; Sunatsuki, Y.; Matsumoto, N. *Chem. Commun.* **2000**, 2113. Kido, T.; Ikuta, Y.; Sunatsuki, Y.; Ogawa, Y.; Matsumoto, N. *Inorg. Chem.* **2003**, *42*, 398.

complexes originates from the neutrality of the L^iMn building unit. Previously, neutral Mn^{III} complexes have essentially been obtained by association of a dianionic Schiff base with a pseudohalide ion in the metal coordination sphere.[8] In addition to this difference, the bridging atom in the present series is included into the ligand, aside from the coordination site, thus allowing self-assembling. The almost identical values of the *J* interaction parameter in the polynuclear systems **2** and **3** originate from the fact that an NCO amido function similarly bridges an equatorial position of one Mn center (through N) to one axial position of the next Mn center (through O) in both complexes. This antiferromagnetic interaction is quite weak in agreement with our previous result showing that coupling of copper and gadolinium ions through the same type of NCO bridge is also weak, 0.6 cm^{-1}, although ferromagnetic.[9]

Acknowledgment. We thank Dr. A. Mari for his contribution to the magnetic measurements. M.-J.R.D. and M.-I.F.G. acknowledge the Ministerio de Ciencia y Tecnologia (MCYT BQU2003-00167) for financial support.

Supporting Information Available: X-ray crystallographic files including the structural data for in CIF format. Additional figures. This material is available free of charge via the Internet at http://pubs.acs.org.

IC0348796